Quantum Electronics **49** (8) 740 – 744 (2019)

https://doi.org/10.1070/QEL16934

Frequency characteristics of a gas coupled-cavity ring laser

I.I. Zolotoverkh, E.G. Lariontsev

Abstract. **Based on a theoretical model describing the lasing dynamics in a gas ring laser (GRL) with coupled cavities, we have investigated the frequency characteristics of radiation. The conditions are found under which an increase in the scale factor is the largest. The regime of frequency locking of counterpropagating waves is studied. It is shown that the lock-in region in a GRL with an antiphase optical coupling of the cavities remains the same as without an additional cavity. The conditions are determined under which multistability of the radiation characteristics arises in a coupled-cavity GRL. In the numerical solution of the equations of the considered theoretical model, three branches of the frequency response are found.**

Keywords: *gas ring laser, coupled cavities, regime of beatings, lock-in regime, multistability of radiation characteristics.*

1. Introduction

Coupled-cavity ring lasers are of interest for fabricating gyroscopes. It was theoretically shown in Refs [1 – 3] that such lasers make it possible to control the intracavity dispersion and create conditions for the occurrence of anomalous dispersion, leading to an increase in the scale factor and sensitivity of a laser gyroscope (LG).

Laser gyroscopes are systems that use optical sensors of angular rotational velocity of two types: ring lasers generating counterpropagating waves with different frequencies inside the laser cavity, and sensors in which the radiation of an external laser is transmitted in opposite directions through the Sagnac interferometer (or ring cavity). Laser gyros with a sensor of the first type are called active, and LGs with a sensor of the second type are called passive. For passive LGs, the possibility of increasing the scale factor using coupled cavities was shown theoretically in [4 – 6].

In this paper we study active LGs. The disadvantage of papers [1 – 3], in which coupled-cavity gas ring lasers (GRLs) were considered, is that they did not take into account the influence on the frequency characteristics of coupling through backscattering and nonlinear interaction of counterpropagating waves in an active medium. To this end, it is necessary to improve the theoretical model of coupled-cavity GRLs, as was done in studies on semiconductor and solid-state ring lasers [7 – 9].

The purpose of this work is a theoretical study of the regimes of beatings and frequency locking in coupled-cavity GRLs.

I.I. Zolotoverkh, E.G. Lariontsev D.V. Skobeltsyn Institute of Nuclear Physics, M.V. Lomonosov Moscow State University, Vorob'evy gory, 119991 Moscow, Russia; e-mail: e.lariontsev@yahoo.com

Received 13 December 2018; revision received 19 February 2019
Kvantovaya Elektronika **49** (8) 740 – 744 (2019)
Translated by I.A. Ulitkin

2. Theoretical model of a GRL

Figure 1 shows a scheme of a coupled-cavity GRL. Inside the main ring cavity containing the active medium (AM), two counterpropagating waves $\tilde{E}_{1,2}$ propagate. The radiation emitted from the main cavity through a partially transmitting coupling mirror M excites the optical fields $\tilde{E}_{c1,c2}$ in the additional ring cavity and returns again to the main cavity through the same mirror.

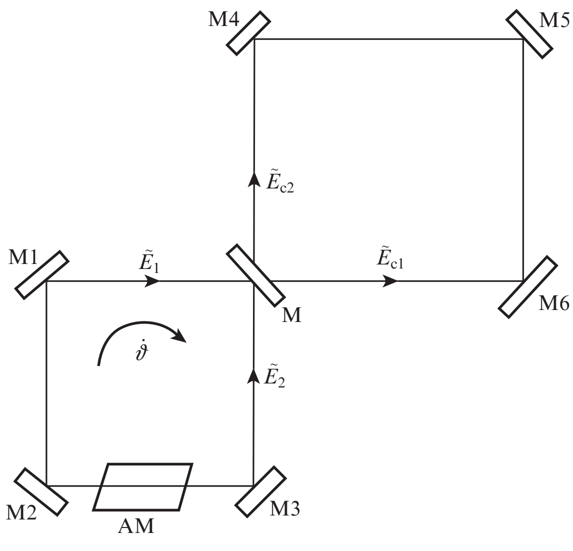

Figure 1. Scheme of a coupled-cavity GRL.

Intracavity fields in the main and additional cavities are written in the form

$$\tilde{E}_{1,2}(t) = E_{1,2}(t)\exp(\mathrm{i}\omega_{\mathrm{n}}t), \quad \tilde{E}_{c1,c2}(t) = E_{c1,c2}(t)\exp(\mathrm{i}\omega_{\mathrm{n}}t), \quad (1)$$

where ω_{n} is the optical frequency of the generated mode. The complex amplitudes $E_{1,2}(t)$ are slow functions of time and change little over the period of optical oscillations. To describe the interaction of counterpropagating waves in a coupled-cavity GRL we will use the following system of ordinary differential equations:

$$\dot{E}_{1,2} = \frac{\Delta\omega_{\rm r}}{2}[\kappa_{1,2}(1+\eta)/\kappa_0 - 1 - \alpha_{1,2}|E_{1,2}|^2 - \beta_{1,2}|E_{2,1}|^2]E_{1,2}$$

$$\pm {\rm i}\frac{\Omega}{2}E_{1,2} + \frac{\rm i}{2}\tilde{m}_{1,2}E_{2,1} + \frac{k_{\rm c}\exp({\rm i}\varphi)}{T}E_{\rm c1,c2}, \quad (2)$$

$$\dot{E}_{\rm c1,c2} = -\frac{\Delta\omega_{\rm c}}{2}E_{\rm c1,c2} \pm {\rm i}\frac{\Omega_{\rm c}}{2}E_{\rm c1,c2} + \frac{k_{\rm c}\exp({\rm i}\varphi + \omega_{\rm n}T_{\rm c})}{T_{\rm c}}E_{1,2}. \quad (3)$$

Equations (2) describe the generation of counterpropagating waves $E_{1,2}$ inside the main cavity taking into account the effect of the fields $E_{c1,c2}$, and equations (3) describe the excitation of counterpropagating waves in the external cavity by waves $E_{1,2}$. Single-mode lasing is considered. In equations (2) and (3), $\Delta\omega_r$ and $\Delta\omega_c$ are the bandwidths of the main and additional cavities; intracavity losses for counterpropagating waves are assumed to be equal. The linear coupling of the counterpropagating waves in the main and additional cavities is determined by the complex coupling coefficients $\tilde{m}_{1,2}$. The coefficients $\kappa_{1,2}$ describe the linear polarisability of the GRL active medium, and the coefficients $\alpha_{1,2}$ and $\beta_{1,2}$ describe its saturation with fields of counterpropagating waves. The coefficient $(1+\eta)/\kappa_0$ is equal to the ratio of the gain to the intracavity losses at the maximum of the gain curve, where $\kappa_0 = \max({\rm Re}\,\kappa_{1,2})$ and η is the excess of the gain over the threshold. The optical coupling coefficients between the fields in the main and additional cavities, $k_c\exp({\rm i}\varphi)/T$ and $k_c\exp({\rm i}\varphi + \omega_n T_c)/T_c$, depend on the amplitude transmittance of the coupling mirror k_c, on the round-trip transit times T and T_c for the light in the main and additional cavities, on the phase shift φ between the reflected and transmitted waves at the coupling mirror, and also on the phase shift per round-trip transit of the additional cavity, $\Phi = \omega_n T_c$.

The sensitivity to rotation is associated with the Sagnac effect: the main and additional cavities due to the rotation exhibit differences between the eigenfrequencies of the counterpropagating waves:

$$\Omega = 8\pi S\dot{\vartheta}/(\lambda L), \quad (4a)$$

$$\Omega_{\rm c} = 8\pi S_{\rm c}\dot{\vartheta}/(\lambda L_{\rm c}), \quad (4b)$$

where S and S_c are the projections of the areas of the main and additional cavities on the axis of rotation; L and L_c are the perimeters of ring cavities; and $\dot{\vartheta}$ is the angular rotation velocity.

The coefficients $\kappa_{1,2}$, $\alpha_{1,2}$, and $\beta_{1,2}$ determining the interaction of counterpropagating waves in the active medium will be calculated on the basis of the GRL vector theory [10, 11], which is valid in the weak field approximation with an arbitrary ratio between the widths of the homogeneous and Doppler lines.

3. Regimes of beatings and frequency locking

3.1. Regime of beatings

Consider the regime of the beating of counterpropagating waves. We assume that the beat frequency ω_b is significantly greater than the coupling of counterpropagating waves through backscattering ($|\omega_b| \gg |\tilde{m}_{1,2}|$). In this case, when solving equations (2) and (3), the coupling coefficients $\tilde{m}_{1,2}$ can be neglected. For simplicity, we restrict ourselves to the case when the additional cavity is insensitive to rotation (the projection of the area vector on the axis of rotation S_c is zero or small).

In the regime of beatings, the time dependence of the complex amplitudes of the counterpropagating waves $E_{1,2}$ will be expressed as

$$E_{1,2}(t) = |E_{1,2}|\exp({\rm i}\omega_{1,2}t), \quad (5)$$

where the moduli of the amplitudes $|E_{1,2}|$ are constant and the beat frequency is $\omega_b = \omega_1 - \omega_2$.

From equations (3) we find

$$E_{\rm c1,c2} = \frac{k_{\rm c}\exp({\rm i}\varphi + {\rm i}\omega_{\rm n}T_{\rm c})/T_{\rm c}}{{\rm i}\omega_{1,2} + \Delta\omega_{\rm c}/2}E_{1,2}. \quad (6)$$

Substituting (6) into equations (2), we obtain the system of equations:

$${\rm i}\omega_{1,2} = [\kappa_{1,2}(1+\eta)/\kappa_0 - 1 - \alpha_{1,2}|E_{1,2}|^2 - \beta_{1,2}|E_{2,1}|^2]\Delta\omega_{\rm r}/2$$

$$\pm {\rm i}\Omega/2 + \frac{A_{\rm c}}{{\rm i}\omega_{1,2} + \Delta\omega_{\rm c}/2}, \quad (7)$$

where $A_c = k_c^2\exp({\rm i}\Phi_c)/(TT_c)$, and $\Phi_c = 2\varphi + \omega_n T_c$.

The imaginary part of equations (7) yields two equations for determining the frequencies $\omega_{1,2}$:

$$\omega_{1,2} = {\rm Im}[\kappa_{1,2}(1+\eta)/\kappa_0 - 1 - \alpha_{1,2}|E_{1,2}|^2 - \beta_{1,2}|E_{2,1}|^2]\Delta\omega_{\rm r}/2$$

$$\pm \Omega/2 - \frac{\omega_{1,2}{\rm Re}\,A_{\rm c}}{\omega_{1,2}^2 + \Delta\omega_{\rm c}^2/4}, \quad (8)$$

and the real part of the equations yields two equations for determining the intensities of the counterpropagating waves $|E_{1,2}|^2$:

$${\rm Re}[\kappa_{1,2}(1+\eta)/\kappa_0 - 1 - \alpha_{1,2}|E_{1,2}|^2 - \beta_{1,2}|E_{2,1}|^2]\Delta\omega_{\rm r}/2$$

$$= -\frac{\Delta\omega_{\rm c}{\rm Re}\,A_{\rm c}/2 + \omega_{1,2}{\rm Im}\,A_{\rm c}}{\omega_{1,2}^2 + \Delta\omega_{\rm c}^2/4}. \quad (9)$$

The system of equations (8) and (9) can be solved by the method of successive approximations. We assume that the following inequality holds:

$$k_{\rm c}^2/(TT_{\rm c}) \gg {\rm Im}[\kappa_{1,2}(1+\eta)/\kappa_0 - 1 - \alpha_{1,2}|E_{1,2}|^2$$

$$-\beta_{1,2}|E_{1,2}|^2]\Delta\omega_{\rm r}/2. \quad (10)$$

In this case, the influence of nonlinear interaction of counterpropagating waves in the active medium on the frequency response of the GRL can be neglected, and equation (8) in the zero approximation takes the form

$$\omega_{1,2} - \frac{\omega_0^2(\omega_{1,2}\cos\Phi_{\rm c} - \sin\Phi_{\rm c}\Delta\omega_{\rm c}/2)}{\omega_{1,2}^2 + \Delta\omega_{\rm c}^2/4} = \pm\Omega/2, \quad (11)$$

where $\omega_0 = k_c/\sqrt{TT_c}$.

When the inequality

$$\omega_{1,2}^2 \ll \Delta\omega_{\rm c}^2/4 \quad (12)$$

is fulfilled, from (11) for the beat frequency we obtain the expression

$$\omega_b = \Omega \frac{\Delta\omega_c^2}{4\omega_0^2 \cos\Phi_c + \Delta\omega_c^2}. \quad (13)$$

It follows from (13) that the dependence of the beat frequency on the angular rotation velocity $\dot{\vartheta}$ is determined by the scale factor

$$K = \frac{\Delta\omega_c^2}{4\omega_0^2 \cos\Phi_c + \Delta\omega_c^2} K_0, \quad (14)$$

where

$$K_0 = 8\pi S/(\lambda L) \quad (15)$$

is the scale factor of the main cavity in accordance with expression (4a).

The expressions for the beat frequency ω_b and the scale factor K include the negative feedback phase (NFB) Φ_c, which depends on two parameters: the phase shift in the additional cavity $\Phi = \omega_n T_c$ and the phase shift φ of the reflected and transmitted waves on the coupling mirror. The NFB phase can be changed from 0 to 2π when adjusting the perimeter of the additional cavity by a value of the order of the wavelength.

We distinguish two particular cases: $\Phi_c = 2\pi p$ (p is an integer), i.e. in-phase optical coupling; and $\Phi_c = 2\pi p + \pi$, i.e. antiphase coupling. In the case of antiphase coupling, the optical coupling between the cavities leads to an increase in losses in the main cavity and to a decrease in the amplitudes $|E_{1,2}|$ of the intracavity fields. The in-phase coupling, on the contrary, compensates for the losses in the main cavity and increases the amplitudes $|E_{1,2}|$ of the intracavity fields.

It follows from (14) that the antiphase optical coupling between the cavities leads to an increase in the scale factor, and the in-phase coupling leads to its reduction. The largest increase in the scale factor occurs when the condition

$$\omega_0^2 = \Delta\omega_c^2/4 \quad (16)$$

is met.

3.2. Lock-in regime

Consider now the lock-in regime, when due to coupling through backscattering, the frequencies of the opposite waves become equal ($\omega_1 = \omega_2 = \omega$). In this regime, the complex amplitudes of the counterpropagating waves $E_{1,2}$ will be expressed as

$$E_{1,2} = A \pm \mathrm{i}B, \quad (17)$$

where A and B are real constant values. From equations (3) we find

$$E_{c1,c2} = \frac{k_c \exp(\mathrm{i}\varphi + \mathrm{i}\omega_n T_c)/T_c}{\Delta\omega_c/2} E_{1,2}. \quad (18)$$

For simplicity, in studying the lock-in regime, the coupling coefficients of counterpropagating waves are given in the form $\tilde{m}_1 = \tilde{m}_2 = m\exp(-\mathrm{i}\pi/2)$. We consider the case of antiphase NFB ($\Phi_c = 2\pi p + \pi$) and the coefficients that determine the polarisation of the medium will be assumed real: $\kappa_1 = \kappa_2 = \kappa$, $\alpha_1 = \alpha_2 = \alpha$, and $\beta_1 = \beta_2 = \beta$. Substituting (18) into equations (2), we obtain the system of equations

$$(A \pm \mathrm{i}B)\Big\{[\kappa(1+\eta)/\kappa_0 - 1 - \alpha(A^2+B^2) - \beta(A^2+B^2)]\frac{\Delta\omega_r}{2} \pm \frac{\mathrm{i}\Omega}{2} + \frac{2\omega_0^2}{\Delta\omega_c}\Big\} + \frac{m}{2}(A \mp \mathrm{i}B) = 0. \quad (19)$$

The real and imaginary parts of these equations can be reduced to the form:

$$AB[\kappa(1+\eta)/\kappa_0 - 1 - \alpha(A^2+B^2) - \beta(A^2+B^2)] \times \frac{\Delta\omega_r}{2} - \frac{\Omega}{2}B^2 + \frac{2\omega_0^2}{\Delta\omega_c}AB + \frac{m}{2}AB = 0. \quad (20)$$

$$AB[\kappa(1+\eta)/\kappa_0 - 1 - \alpha(A^2+B^2) - \beta(A^2+B^2)] \times \frac{\Delta\omega_r}{2} + \frac{\Omega}{2}A^2 + \frac{2\omega_0^2}{\Delta\omega_c}AB - \frac{m}{2}AB = 0. \quad (21)$$

Subtracting (21) from (20), we obtain the equation

$$\Omega(A^2 + B^2) = 2mAB. \quad (22)$$

Expressing A and B through the amplitude E_0 and phase ψ, we rewrite (22) in the form

$$\frac{\Omega}{m} = \sin(2\psi). \quad (23)$$

It follows from (23) that the lock-in regime exists in the region

$$-m \leqslant \Omega \leqslant m. \quad (24)$$

In accordance with (24), the optical coupling between the cavities does not affect the width of the lock-in region. In the GRL with antiphase NFB, the lock-in region remains the same as without an additional cavity.

3.3. GRL frequency characteristics

In the zero approximation (without taking into account the nonlinear coupling of counterpropagating waves in the active medium), the dependence of the beat frequency $f_b = \omega_b/2\pi$ on the frequency nonreciprocity $\Omega/2\pi$ of the main ring cavity can be calculated using equations (11). Analytical formulae for the corrections in the first approximation to the beat frequency, which take into account the influence of the coupling of counterpropagating waves through backscattering and nonlinear coupling in the active medium, will not be derived in this work. These corrections will be considered on the basis of a numerical solution of the system of equations (2) and (3).

In the numerical solution of equations (2) and (3), the coefficients $\kappa_{1,2}$, which describe the linear polarisability of the GRL active medium, and the saturation coefficients $\alpha_{1,2}$ and $\beta_{1,2}$ will be calculated using the formulae given in [10, 11] for a 0.63-μm ring He–Ne laser at the $3s_2$–$2p_4$ transition of neon. Consider a single-isotope laser at a pressure of p = 700 Pa with a Doppler line width of 800 MHz, a uniform transition line width of 357 MHz, an upper level width of 32 MHz, and a lower level width of 85 MHz. We assume that the magnetic field H, which provides the splitting of the magnetic sublevels of neon, is absent ($H = 0$).

First, we consider the situation when condition (16) is satisfied for coupled-cavity GRLs. As already noted, in the case of antiphase optical coupling one should expect that the scale factor defined by formula (14) will be maximum. Let us choose the following parameters of the cavities: the perimeters of the main and additional cavities are $L = 10$ cm and $L_c = 40$ cm, and the losses per round-trip of these cavities are 0.005 and 0.0075, respectively. At the amplitude transmittance of the coupling mirror $k_c = 0.0019$, condition (16) is exactly satisfied for the GRL with the specified parameters of coupled cavities. With such values of the parameters, Fig. 2 shows the dependence of the beat frequency f_b on the frequency nonreciprocity $\Omega/2\pi$ of the main ring cavity. The solid curve in Fig. 2 corresponds to the beat frequency in the zero approximation, calculated using formulae (11). The dots show the results obtained on the basis of the numerical solution of equations (2) and (3) with the coupling coefficients of the counterpropagating waves $\tilde{m}_{1,2} = m\exp(-i\pi/2)$ ($m/2\pi = 100$ Hz) when the gain exceeds the threshold $\eta = 0.5$. The calculation was performed for a GRL with an optical coupling close to the antiphase one with $\Phi_c = 1.0091\pi$. With this phase of optical coupling Φ_c, as shown by the numerical solution of equations (2) and (3), the scale factor in the presence of the coupling of the counterpropagating waves turns out to be maximal. The largest increase in the scale factor ($K/K_0 = 1400$) in this case occurs at $\Omega/2\pi = 0.66$ kHz.

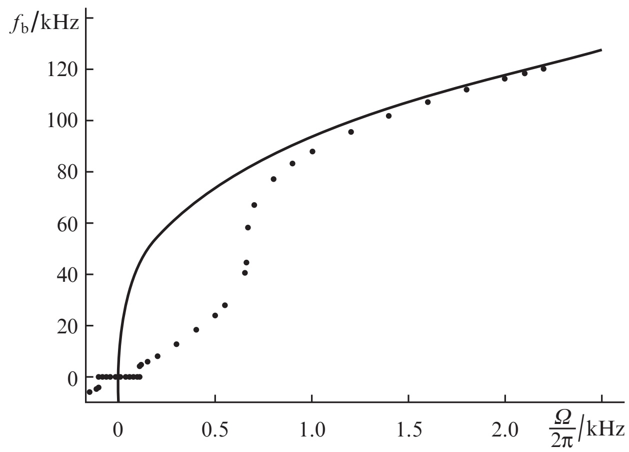

Figure 2. Dependence of the beat frequency of counterpropagating waves on the frequency nonreciprocity $\Omega/2\pi$ in a GRL with an optical coupling close to the antiphase one when condition (16) is satisfied. The solid curve corresponds to the beat frequency ω_b calculated by formulae (11). The dots show the results obtained in the numerical solution of equations (2) and (3). The values of the parameters of the cavities are given in the text.

One can see from Fig. 2 that for low frequency nonreciprocities, in the region of -100 Hz $\leqslant \Omega/2\pi \leqslant 100$ Hz, the frequencies of counterpropagating waves are locked in. The width of the lock-in region is determined by the modulus of the coupling coefficient of the counterpropagating waves, m, and does not depend on the optical coupling between the cavities. At the boundary of the lock-in region, the beat frequency changes abruptly by 4.35 kHz.

3.4. Frequency hysteresis

In Section 3.3, the frequency characteristics of the GRL were considered in the case of optical coupling satisfying the condition $k_c^2/(TT_c) = \Delta\omega_c^2/4$. As shown in [12], when the inequality

$$k_c^2/(TT_c) > \Delta\omega_c^2/4 \qquad (25)$$

holds for coupled-cavity GRLs, due to spontaneous phase symmetry breaking, new branches of the frequency characteristic appear. Let the GRL have the following parameters: the perimeters of the main and additional cavities are $L = 10$ cm and $L_c = 40$ cm and the losses per round-trip in these cavities are 0.0049 and 0.00748, respectively. In this case, with the amplitude transmittance of the coupling mirror $k_c = 0.0019$, inequality (25) is satisfied. With such values of parameters, Fig. 3 shows the dependence of the beat frequency f_b on the frequency nonreciprocity $\Omega/2\pi$ of the main ring cavity. The solid curve in Fig. 3 corresponds to the beat frequency in the zero approximation, calculated using formulae (11). The dots show the results obtained on the basis of the numerical solution of equations (2) and (3) with the coupling coefficients of the counterpropagating waves $\tilde{m}_{1,2} = m\exp(-i\pi/2)$ ($m/2\pi = 100$ Hz) at $\eta = 0.5$ and the values of the parameters of the active medium specified above for a single-isotope He–Ne laser at a pressure $p = 700$ Pa. The calculation was performed for a GRL with an optical coupling close to the antiphase one at $\Phi_c = 1.009208\pi$.

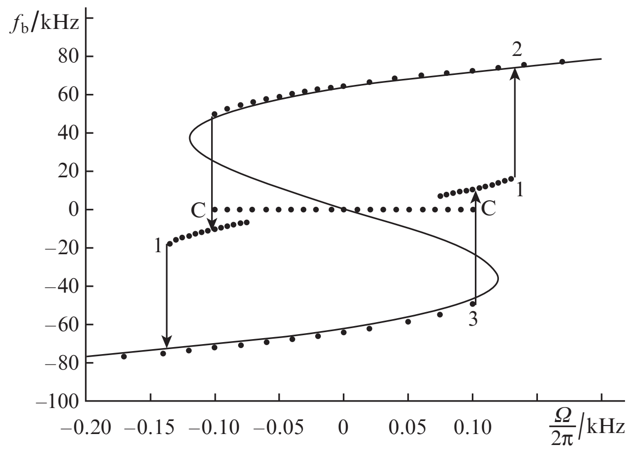

Figure 3. Three branches of the frequency response for a GRL with an optical coupling close to the antiphase one when the condition (25) is satisfied. The solid curve corresponds to the beat frequency ω_b calculated by formulae (11). The dots show the results obtained in the numerical solution of equations (2) and (3). The values of the parameters of the cavities are given in the text.

One can see from Fig. 3 that the frequency response has three branches with numbers 1, 2 and 3. At the exit from the frequency lock-in region C with frequency nonreciprocity $\Omega/2\pi > 100$ Hz, the regime of beatings occurs on branch 1. On the right boundary of branch 1 with $\Omega/2\pi > 130$ Hz, there occurs a transition to the regime of beatings on branch 2. On the left boundary of branch 2, at $\Omega/2\pi < -100$ Hz, a transition to branch 1 is observed. On the left boundary of branch 1, at $\Omega/2\pi < -136$ Hz, the GRL undergoes a transition to the regime of beatings on branch 3.

4. Conclusions

We have studied the frequency characteristics of coupled-cavity GRLs on the basis of a theoretical model that describes the lasing dynamics with allowance for the coupling through backscattering and the nonlinear interaction of counterpropagating waves in an active medium. It is shown that the antiphase optical coupling of the cavities leads to an increase in the scale factor. The greatest increase in this coefficient occurs when condition (16) is satisfied. In the case of coupled cavities, a strongly nonlinear dependence of the beat frequency on the rotational velocity arises, which creates considerable difficulty for the practical use of the effect of increasing the scale factor. The regime of of frequency locking of counterpropagating waves is investigated. It is found that for a GRL with antiphase NFB, the lock-in region remains the same as without an additional cavity. The conditions are found under which multistability of the radiation characteristics arises in a coupled-cavity GRL. In solving numerically equations (2) and (3) within the framework of the considered theoretical model, three branches of the frequency response are found.

References

1. Schaar J.E., Yum H.N., Shahriar S.M. *Proc. SPIE*, **7949**, 794914 (2011).
2. Han X., Luo H., Qu T., Wang Z., Yuan J., Bin Z. *J. Opt*., **16**, 125401 (2014).
3. Wang Z., Yuan B., Xiao G., Fan Z., Yuan J. *Appl. Opt*., **54**, 9568 (2015).
4. Smith D.D., Chang H., Myneni K., Rosenberger A.T. *Phys. Rev. A*, **89**, 053804 (2014).
5. Peng C., Li Z., Xu A. *Opt. Express*, **15**, 3864 (2007).
6. Terrel M.A., Digonnet M.J.F., Fan S. *Proc. SPIE*, **7612**, 76120B (2010).
7. Ermakov V., Beri S., Ashour M., Danckaert J., Docter J., Bolk J., Leijtens X.J.M., Verschaffelt G. *IEEE J. Quantum Electron*., **48**, 129 (2012).
8. Zolotoverkh I.I., Lariontsev E.G., Firsov V.V., Chekina S.N. *Quantum Electron.*, **48**, 1 (2018) [*Kvantovaya Elektron*., **48**, 1 (2018)].
9. Zolotoverkh I.I., Lariontsev E.G. *Quantum Electron*., **48**, 510 (2018) [*Kvantovaya Elektron*., **48**, 510 (2018)].
10. Khromykh A.M., Yakushev A.I. *Sov. J. Quantum Electron.*, **7**, 13 (1977) [*Kvantovaya Elektron*, **4**, 27 (1977)].
11. Savel'ev I.I., Khromykh A.M., Yakushev A.I. *Sov. J. Quantum Electron.*, **9**, 682 (1979) [*Kvantovaya Elektron.*, **6**, 1155 (1979)].
12. Zolotoverkh I.I., Lariontsev E.G. *Quantum Electron*., **49** (7), 653 (2019) [*Kvantovaya Elektron*., **49** (7), 653 (2019)].